



# Unexpected stability of CuO/Cryptomelane catalyst under Preferential Oxidation of CO reaction conditions in the presence of CO<sub>2</sub> and H<sub>2</sub>O

A. Davó-Quiñonero\*, D. Lozano-Castelló, A. Bueno-López

MCMA group, Inorganic Chemistry Department, University of Alicante, Carretera San Vicente s/n. E03080, Alicante, Spain



## ARTICLE INFO

### Article history:

Received 13 April 2017

Received in revised form 26 May 2017

Accepted 31 May 2017

Available online 1 June 2017

### Keywords:

PROX

Copper

Cryptomelane

CO oxidation

H<sub>2</sub> purification

PEMFC

## ABSTRACT

The catalytic activity of CuO/Cryptomelane for the preferential oxidation of CO in H<sub>2</sub>-rich streams has been studied in the absence and presence of H<sub>2</sub>O and CO<sub>2</sub>, paying special attention to the catalyst stability and to changes on its physical-chemical properties under CO-PROX reaction conditions.

For fresh CuO/cryptomelane catalyst, the presence of CO<sub>2</sub> and/or H<sub>2</sub>O in the CO-PROX feed partially inhibits CO oxidation due to chemisorption of H<sub>2</sub>O and CO<sub>2</sub> on the catalyst. H<sub>2</sub>O chemisorption on CuO/Cryptomelane is stronger than CO<sub>2</sub> chemisorption, and simultaneous CO<sub>2</sub> and H<sub>2</sub>O adsorption has a synergistic effect that enhances co-adsorption and significantly hinders CO oxidation.

On the contrary, the presence of CO<sub>2</sub> + H<sub>2</sub>O in the CO-PROX reaction mixture has a positive effect in the CuO/Cryptomelane stability upon several consecutive reaction cycles in the 25–200 °C range. XRD showed that chemisorbed CO<sub>2</sub> + H<sub>2</sub>O species partially prevent the catalyst deactivation due to cryptomelane reduction to hausmannite (Mn<sub>3</sub>O<sub>4</sub>) under the strongly reductive environment of the CO-PROX reaction, and H<sub>2</sub>-TPR and Raman spectroscopy characterisation support that the cryptomelane structure is less damaged under CO-PROX conditions in the presence of CO<sub>2</sub> and H<sub>2</sub>O than in the absence of these species. Therefore, interestingly under CO<sub>2</sub> + H<sub>2</sub>O environment (realistic CO-PROX conditions) CuO/Cryptomelane catalyst performs an improved catalytic activity.

© 2017 Elsevier B.V. All rights reserved.

## 1. Introduction

The PREFERENTIAL OXidation of CO (CO-PROX) reaction is an efficient strategy to remove the residual CO content in H<sub>2</sub>-rich streams produced by steam reforming of hydrocarbons coming from the water-gas shift reactor. This methodology permits utilisation of proton exchange membrane (PEM) fuel cells with current H<sub>2</sub>-production technologies to provide stationary and portable power [1,2]. Basically, CO-PROX is a competitive process in which a stoichiometric content of O<sub>2</sub> is supplied to the gas mixture, and an appropriate catalyst should accelerate selectively CO oxidation to CO<sub>2</sub> with, ideally, no H<sub>2</sub> consumption [3].

Previous research done into this subject has agreed to claim the CuO/CeO<sub>2</sub> and derivate catalysts as promising materials to overcome the challenging requirements towards CO-PROX reaction in terms of activity and selectivity. Nevertheless, this catalyst is based in a rare-earth metal oxide and, thus, coming from resources involved in a serious environmental, political and social problematic associated to their extraction, purification and use.

[4]. Although novel procedures are being investigated to reduce the mining processes by promoting the sustainable recycling of these materials, their availability and supply in extended use are still unclear and polemic matters. So, despite the properties of rare-earth elements are being unique, they should be gradually substituted if alternative materials are found to perform similarly for certain applications, such as catalysis.

In this particular context, manganese oxides result highly interesting given their abundance and variety, low cost, environmental compatibility and non-toxicity [5]. They have traditionally been combined to copper, forming the hopcalite catalyst (CuMn<sub>2</sub>O<sub>4</sub>), which has been used since World War I as an effective CO oxidation catalyst in masks and respiratory protection [6,7]. Its catalytic activity has been related to the existence of flexible valences Cu<sup>+</sup>/Cu<sup>2+</sup> and Mn<sup>3+</sup>/Mn<sup>4+</sup> in permanent equilibrium and to its low crystallinity [6]. However, it is still a subject of research to discern which is the role of each species in the catalytic steps, and how to control and prevent the severe deactivation process that occurs during reaction.

Among the wide range of manganese oxides, the cryptomelane-based oxide (K<sub>x</sub>Mn<sub>8</sub>O<sub>16</sub>) has been pointed out as a promising material for catalysis applications [8]. This material consists in an open tunneled network formed by double chains of corner-sharing

\* Corresponding author.

E-mail address: [arantxa.davo@ua.es](mailto:arantxa.davo@ua.es) (A. Davó-Quiñonero).

$\text{MnO}_6$  octahedra ( $2 \times 2$ ), which gives rise to its typical denomination as Octahedral Molecular Sieve  $2 \times 2$  (OMS-2). The channel size is  $0.46 \times 0.46$  nm, where interstitial potassium species and water ions are hosted, compensating the charge imbalance generated into the mixed valence of manganese, typically around 3.8 by the presence of  $\text{Mn}^{4+}$ ,  $\text{Mn}^{3+}$  and minor  $\text{Mn}^{2+}$  [9].

Particularly, cryptomelane has been thoroughly studied as a catalyst for oxidation reactions and has demonstrated an excellent activity, which has been related to its high oxygen mobility and its redox properties [10,11]. As well, the modification of cryptomelane with transition and noble metals has been reported to produce improvements on its catalytic activity when Co [12,13], Ce [14,15], Cu [16–18], Ag [19–21] or Au [14,22] among others were incorporated. From all of them, the best results were obtained when copper was the doping element, associated to the strong Cu-Mn interaction and synergistic effect on the reducibility [12,13].

On the other hand, deposition of finely dispersed CuO nanoparticles on cryptomelane surface has also been reported to be positive for CO oxidation [23]. Following this approach, in our previous study we tested a CuO/Cryptomelane catalyst in CO-PROX reaction with a  $\text{CO} + \text{H}_2 + \text{O}_2$  gas mixture, and an exceptional performance was found [24]. However, its catalytic activity lowered in successive cycles of reaction, despite regeneration steps were conducted between cycles. Such deactivation was associated to partial collapse of cryptomelane structure produced by potassium segregation and copper sintering under CO-PROX reaction conditions. Despite this loss of activity, the remaining activity of CuO/Cryptomelane catalyst showed a good potential for CO-PROX oxidation under the reaction conditions of that study.

The effect of  $\text{CO}_2$  and  $\text{H}_2\text{O}$  in the CO-PROX reaction feed in the activity, selectivity and stability of CuO/Cryptomelane was not evaluated in our previous study [24], and it is known the detrimental effect of these inhibitors in many CO-PROX catalysts, such as CuO/Ceria [25]. The study from Hernández et al. [16] was pioneer in undergoing CO-PROX real conditions using Cryptomelane. These authors evaluated the activity of Cu-modified cryptomelane for CO-PROX reaction with the addition of  $\text{CO}_2$ ,  $\text{H}_2\text{O}$  and  $\text{CO}_2 + \text{H}_2\text{O}$  in the reaction mixture, concluding that  $\text{CO}_2$  partially inhibits the activity while  $\text{H}_2\text{O}$  inhibits or enhances the activity depending on the reaction temperature. The inhibiting effect of  $\text{CO}_2$  and  $\text{H}_2\text{O}$  was attributed to the blockage of CO chemisorption sites while the positive effect of  $\text{H}_2\text{O}$  above a critical temperature was explained appealing to the thermodynamics of parallel reactions that could take place in presence of water, such as the Reverse Water Gas Shift reaction [26], and to the formation of labile intermediates of fast desorption by means of the surface hydroxyl groups. As far as we know, the stability of CuO/Cryptomelane catalysts under CO-PROX reaction conditions including  $\text{CO}_2$  and  $\text{H}_2\text{O}$  in the reaction mixture has not been studied so far, and this is a critical issue for the potential application of this promising catalysts in real devices. Therefore, the goal of this study is to analyse the stability of CuO/Cryptomelane catalyst under realistic CO-PROX conditions including  $\text{CO}_2$ ,  $\text{H}_2\text{O}$  and  $\text{CO}_2 + \text{H}_2\text{O}$  in the gas mixture, not only paying attention to the effect of these species on the chemical processes occurring under reaction conditions but also to changes on the physical-chemical properties of the catalyst in consecutive reaction tests.

## 2. Experimental details

### 2.1. Catalysts preparation

Synthetic cryptomelane was prepared using the previously described reflux method [27]. To this end, 11 g of manganese (II) acetate were dissolved in 40 g of water and the pH of the solution was fixed at 5 using glacial acetic acid. Then, the solution was

heated and maintained at the boiling temperature under reflux for 30 min. After that, a solution of 6.5 g of potassium permanganate dissolved in 150 ml of water was added, and the mixture was kept under reflux by vigorous stirring for 24 h. The solid was filtered, washed with distilled water until neutral pH and dried at 120 °C overnight. Finally, the sample was calcined in air at 450 °C for 2 h using a heating ramp of 5 °C/min.

The CuO/Cryptomelane catalyst was prepared with 5 wt.% of copper by incipient wetness impregnation of cryptomelane with a copper(II) nitrate trihydrate (Panreac) water solution. The impregnated solid was dried at 110 °C overnight and calcined in air at 400 °C for 5 h using a heating ramp of 5 °C/min.

### 2.2. CO-PROX catalytic tests

To perform CO-PROX experiments, 150 mg of CuO/Cryptomelane were placed in a U-shaped reactor with 16 mm inner diameter and the gas mixture of 2% CO, 2%  $\text{O}_2$ , 30%  $\text{H}_2$  and He balance was fed to the reactor. The  $\text{O}_2$  excess with regard to CO was  $\lambda = 2$  (being  $\lambda = 1$  for stoichiometric CO- $\text{O}_2$  conditions). The catalytic tests were performed using a heating rate of 2 °C/min from 25 to 200 °C and a total gas flow rate of 100 ml/min that was set by means of Mass Flow Controllers (Bronkhorst). The exhaust gases were analysed by gas chromatography in an Agilent Technologies 6890N device equipped with a CTRI column operating at 80 °C and a TCD detector.

In order to study the effect of  $\text{CO}_2$  and  $\text{H}_2\text{O}$  in the CO-PROX catalytic activity of the prepared CuO/Cryptomelane, different catalytic tests were performed adding 9%  $\text{CO}_2$  or 5%  $\text{H}_2\text{O}$  or 9%  $\text{CO}_2 + 5\%$   $\text{H}_2\text{O}$  to the reactant gas mixture.  $\text{CO}_2$  was fed to the gas mixture using an additional mass flow controller and  $\text{H}_2\text{O}$  was introduced in the gas mixture passing the gas stream through a gas saturator at 33 °C.

Consecutive catalytic cycles were performed with the same parcel of catalyst under each gas mixture in order to evaluate the stability of the catalyst. After the first run, the reactor was cooled down to room temperature under He atmosphere and a new catalytic cycle was conducted, repeating the experimental conditions of each series for four consecutive runs.

### 2.3. Temperature programmed experiments

In order to study the chemical adsorption of  $\text{CO}_2$  and  $\text{H}_2\text{O}$  on CuO/Cryptomelane catalysts, temperature programmed desorption (TPD) experiments were performed. 80 mg of catalyst were placed in a tubular quartz reactor and were pretreated at 400 °C for 30 min in a 100 ml/min flow of Ar. Then, a saturation step with the selected gas was carried out, which consisted of heating the catalyst at 150 °C and keeping that temperature for 1 h under 100 ml/min of 10%  $\text{CO}_2/\text{Ar}$  (for  $\text{CO}_2$ -TPD), 5%  $\text{H}_2\text{O}/\text{Ar}$  (for  $\text{H}_2\text{O}$ -TPD) or 10%  $\text{CO}_2 + 5\%\text{H}_2\text{O}/\text{Ar}$  (for  $\text{CO}_2 + \text{H}_2\text{O}$ -TPD). After that, the gas mixture was switched to Ar, and once the  $\text{CO}_2$  and  $\text{H}_2\text{O}$  signals reached the baseline, the reactor was heated up to 650 °C following a ramp of 10 °C/min in 100 ml/min of Ar. The outlet gases were analysed with a mass spectrometer (Pfeiffer Vacuum, model OmniStar).

Experiments of temperature programmed reduction with  $\text{H}_2$  ( $\text{H}_2$ -TPR) were performed using a Micromeritics Pulse ChemiSorb 2705 device. 40 mg of catalyst were placed in a U-shaped reactor and the temperature was increased from room temperature up to 900 °C with a heating rate of 10 °C/min in 40 ml/min of 5%  $\text{H}_2$  in Ar. The TCD signal was calibrated using a CuO pattern provided by the manufacturer of the equipment.

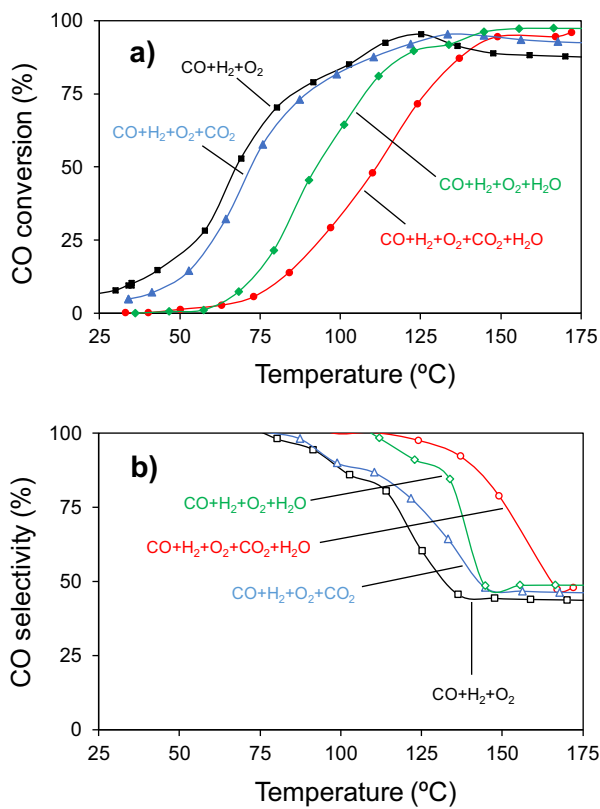


**Fig. 1.** CO-PROX experiments performed with fresh catalyst (first run for each gas mixture) under gas mixtures of different composition. (a) CO conversion and (b) CO selectivity. 150 mg of catalyst, 100 ml/min; 2 °C/min; gas concentrations: 2% CO, 2% O<sub>2</sub>, 30% H<sub>2</sub>, 9% CO<sub>2</sub>, 5% H<sub>2</sub>O and He balance.

#### 2.4. Characterisation techniques

X-ray diffractograms were recorded in a Bruker D8-Advance diffractometer provided with Göbel mirror, using Cu K $\alpha$  radiation ( $\lambda=1.540598\text{ \AA}$ ). Diffractograms were recorded at  $2\theta$  between  $10^\circ$  and  $90^\circ$ , with a step size of  $0.05^\circ$  and a time of 3 s per step. Raman spectra were recorded in a Jasco NRS-5100 dispersive Raman using laser source of 632.8 nm and a 4-stage Peltier cooled CCD detector. The Raman signal was collected using a 20 x (0.45 NA) objective. The laser power, calibrated on the sample, was kept close to 1.8 mW. The Raman shift was calibrated using the  $520.7\text{ cm}^{-1}$  line of crystalline silicon prior to the sample analysis.

### 3. Results and discussion

#### 3.1. Catalytic CO-PROX reaction tests

Fig. 1 shows the CO conversion (Fig. 1a) and CO selectivity (Fig. 1b) profiles in the ramp experiments conducted in CO-PROX conditions for the fresh CuO/Cryptomelane catalyst (first run) under the different atmospheres tested.

According to Fig. 1, the gas mixture composition strongly affects the catalytic activity. The catalyst showed the best performance when tested under CO + H<sub>2</sub> + O<sub>2</sub> mixture, reaching its maximum CO conversion of 95% at 125 °C and keeping after that temperature a stable conversion of 88%. Such CO conversion decay coincides with a loss of CO oxidation selectivity towards the competitive reaction of H<sub>2</sub> oxidation, which reaches an acceptable constant value of 44% (being 50% the maximum selectivity that can be achieved given the O<sub>2</sub> stoichiometric excess,  $\lambda=2$ ). This was the expected behaviour of this catalyst for these experimental conditions and is in good

agreement with the behaviour previously reported on literature [11,16].

The addition of CO<sub>2</sub> to the reactant mixture slightly decreases the catalytic activity, shifting the CO conversion and CO selectivity profiles towards higher temperatures. The inhibitor effect of CO<sub>2</sub> in many CO-PROX catalysts is well-known [16,28], but in this case, our CuO/Cryptomelane catalyst is only minimally affected. On the contrary, results on Fig. 1 evidence that H<sub>2</sub>O strongly affects CO oxidation, delaying the CO oxidation curve about 25 °C, and the experiment performed with CO + H<sub>2</sub> + O<sub>2</sub> + CO<sub>2</sub> + H<sub>2</sub>O reveals a synergy between the CO<sub>2</sub> and H<sub>2</sub>O inhibiting effects.

Some authors suggested that the presence of H<sub>2</sub>O and/or CO<sub>2</sub> in the CO-PROX reaction mixture does not affect the mechanism of reaction for transition metal (Co, Cr, Cu, Ni, Zn) catalysts supported on oxides with very different nature (MgO, La<sub>2</sub>O<sub>3</sub>, SiO<sub>2</sub>-Al<sub>2</sub>O<sub>3</sub>, CeO<sub>2</sub>, Ce<sub>0.63</sub>Zr<sub>0.37</sub>O<sub>2</sub>), as CO selectivity profile is not modified in any case, just shifting in temperature in the same way than CO conversion [29]. These conclusions are also in agreement with those of Hernández et al. [16] for Cu-modified Cryptomelane CO-PROX catalysts, but these authors additionally reported the contribution of parallel reactions involving H<sub>2</sub>O above a certain temperature.

Assuming that the inhibition processes can be associated to chemisorption of H<sub>2</sub>O and CO<sub>2</sub> on the CuO/Cryptomelane catalyst, our results indicate that H<sub>2</sub>O chemisorption on CuO/Cryptomelane is stronger than CO<sub>2</sub> chemisorption. H<sub>2</sub>O chemisorption could take place both in the external surface of cryptomelane and/or into the channels. External chemisorption of H<sub>2</sub>O (and CO<sub>2</sub>) is expected to compete with CO chemisorption, while H<sub>2</sub>O chemisorption into the channels will increase the amount of structural water decreasing the population of oxygen vacancies and oxygen mobility.

According to literature results obtained for other CO-PROX catalysts [29], surface CO<sub>2</sub> chemisorption probably leads to the formation of mono- and/or bidentate carbonates on the catalyst surface, H<sub>2</sub>O is expected to lead to the formation of hydroxyl groups, and simultaneous CO<sub>2</sub> and H<sub>2</sub>O chemisorption will probably form a mixture of carbonate and bicarbonate species [30]. Unfortunately, all our attempts to identify such chemisorbed species by *in situ* DRIFTS experiments failed due to the high adsorption of IR radiation by the CuO/Cryptomelane catalyst because of its dark black colour.

In order to check the stability of the CuO/Cryptomelane catalyst under the catalytic conditions tested, four consecutive cycles of reaction were carried out (without any regeneration treatment between cycles). The CO conversion and selectivity profiles obtained were qualitatively similar to those compiled in Fig. 1, and only changed the temperatures depending on the gas mixture and run number. Fig. 2 compiles the temperatures for 50% CO conversion in these experiments.

In accordance to our previous conclusions [24], the catalytic activity in CO + H<sub>2</sub> + O<sub>2</sub> decreases after the first run, and this was attributed to the segregation of crystalline phases (hausmannite (Mn<sub>3</sub>O<sub>4</sub>) and/or hopcalite (CuMn<sub>2</sub>O<sub>4</sub>)), with the segregation of potassium to the surface and decrease in the reducibility of copper cations. Fig. 2 shows that the effect in CO oxidation of CO<sub>2</sub> in the reaction atmosphere is quite small.

On the contrary, deactivation in consecutive cycles occurs more gradually in the presence of H<sub>2</sub>O, leading to a steady state in the fourth cycle similar to that achieved with CO + H<sub>2</sub> + O<sub>2</sub> (with and without CO<sub>2</sub>). Therefore, the presence of H<sub>2</sub>O seems to affect the kinetics of changes occurring on the catalyst leading to partial deactivation. Such positive impact is even more evident when CO<sub>2</sub> and H<sub>2</sub>O are added at the same time, since the catalyst reaches a stable behaviour after the third cycle with a T<sub>50</sub> temperature lower to that achieved under all other gas mixtures tested. In the presence of CO<sub>2</sub> + H<sub>2</sub>O, the catalytic activity is clearly inhibited on the first run, but the moderate deactivation occurring along further cycles leads

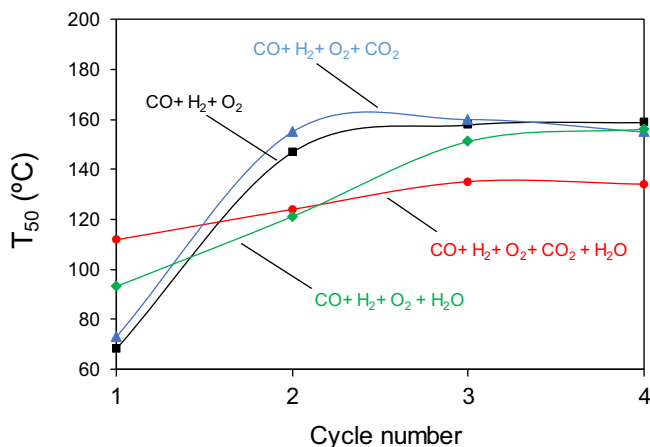


**Fig. 2.** Temperature for 50% of CO conversion at each cycle of reaction under gas mixtures of different composition.

to the best performance after four cycles of reaction. Hence, in these conditions,  $\text{CO}_2$  is facilitating  $\text{H}_2\text{O}$ -cryptomelane interaction, which is being positive for the maintenance of the catalyst integrity. Thus, despite the negative blocking of the catalyst surface by  $\text{CO}_2$  and  $\text{H}_2\text{O}$  and the consequent initial inhibition of the catalytic activity, the incorporation of  $\text{CO}_2$  and  $\text{H}_2\text{O}$  is, in the end, positive to perform CO-PROX in CuO/Cryptomelane in further reaction cycles.

### 3.2. Temperature programmed desorption (TPD) experiments

In order to study the  $\text{CO}_2$  and  $\text{H}_2\text{O}$  chemisorption on CuO/Cryptomelane, TPD experiments were conducted after saturation of the catalyst with  $\text{CO}_2$  ( $\text{CO}_2$ -TPD),  $\text{H}_2\text{O}$  ( $\text{H}_2\text{O}$ -TPD), and  $\text{CO}_2 + \text{H}_2\text{O}$  ( $\text{CO}_2 + \text{H}_2\text{O}$ -TPD). Additionally, a control experiment was carried out omitting the saturation step previous to TPD. The control experiment allows discerning the effect of the saturation steps from the inherent decomposition of the fresh material. Fig. 3 shows the results obtained in all TPD experiments conducted, following by mass spectrometry the m/z signals 44, 18 and 32, corresponding to  $\text{CO}_2$ ,  $\text{H}_2\text{O}$  and  $\text{O}_2$ , respectively.

Two regions must be distinguished on Fig. 3, below and above  $500^\circ\text{C}$  approximately. Cryptomelane structure starts decomposing to  $\text{Mn}_2\text{O}_3$  at temperatures around  $500^\circ\text{C}$ , the actual temperature depending on the atmosphere and particle size [31]. This is consistent with the release of  $\text{O}_2$  observed in Fig. 3c, and previous saturation of the catalysts with  $\text{CO}_2$  and/or  $\text{H}_2\text{O}$  has a minor effect on the release of  $\text{O}_2$  in the experimental conditions of these experiments. Below  $500^\circ\text{C}$ , the cryptomelane structure is maintained but a loss of the water bounded to the nanofibers takes place together with desorption of the chemisorbed species.

After saturation with  $\text{CO}_2$ , a  $\text{CO}_2$  evolution peak centred at  $215^\circ\text{C}$  is observed on the TPD profile (Fig. 3a), which is associated to the decomposition of carbonates formed during the saturation step. The intensity of this peak increases drastically upon saturation with a mixture of  $\text{CO}_2 + \text{H}_2\text{O}$ , indicating that the presence of  $\text{H}_2\text{O}$  significantly enhances  $\text{CO}_2$  chemisorption.

Besides, it can be discerned in Fig. 3b two types of chemisorbed  $\text{H}_2\text{O}$  species that are desorbed in the ranges  $150\text{--}300^\circ\text{C}$  and  $300\text{--}375^\circ\text{C}$ , corresponding to the evolution of surface-related water and water bounded inside the  $2 \times 2$  tunnels, respectively. On the other hand,  $\text{CO}_2$ -TPD and  $\text{H}_2\text{O}$ -TPD experiments show that cryptomelane has a clear preference towards water interaction and is capable to chemisorb water in the narrow tunnel with strong adsorption potential due to the micropore filling, which is in agreement with the study of Kijima et al. [32].

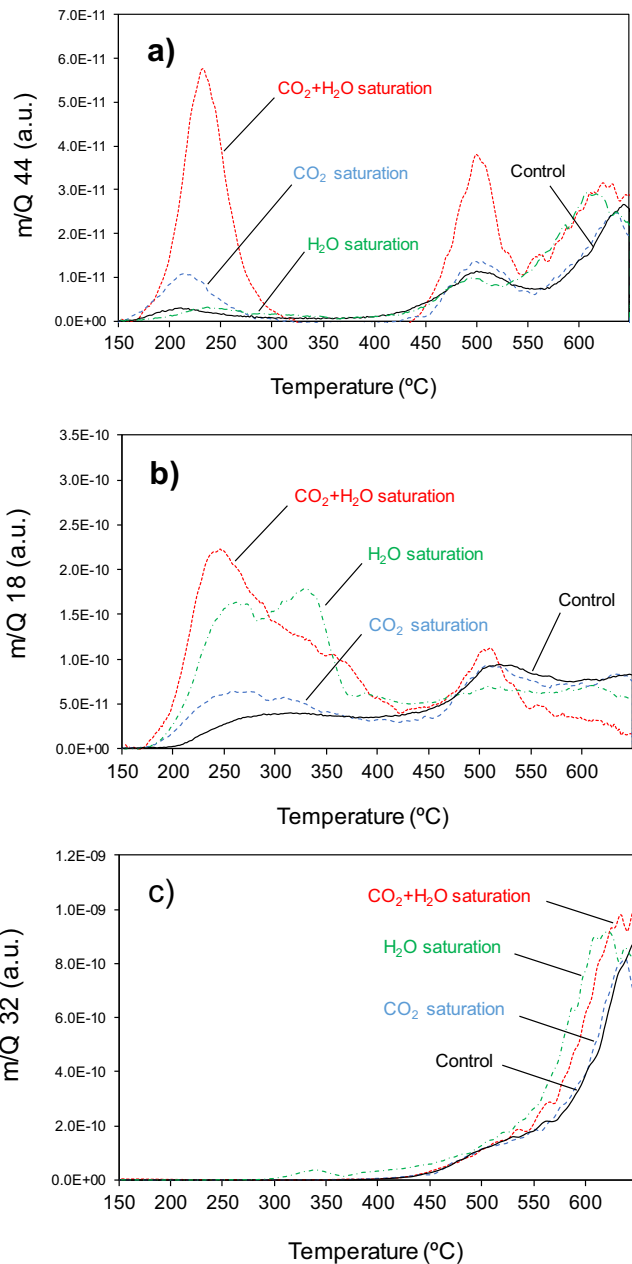


**Fig. 3.** TPD experiments performed in Ar after saturation of the CuO/Cryptomelane catalyst with  $\text{CO}_2$ ,  $\text{H}_2\text{O}$ , or  $\text{CO}_2 + \text{H}_2\text{O}$  (control = no previous saturation). (a)  $\text{CO}_2$  release, (b)  $\text{H}_2\text{O}$  release and (c)  $\text{O}_2$  release.

When  $\text{CO}_2$  and  $\text{H}_2\text{O}$  are added simultaneously in the saturation step, the emission profiles for the signals 44 and 18 change in a great measure, displaying a coupled  $\text{CO}_2$  and  $\text{H}_2\text{O}$  evolution and evidencing the magnification of the chemisorption capacity of cryptomelane towards these species when added together rather than in separate environments. Below  $450^\circ\text{C}$ , the sharp  $\text{CO}_2$  peak can be matched to the  $\text{H}_2\text{O}$  evolution in the same temperature window, which is associated to the desorption of bicarbonate species, which are thermodynamically less stable and more labile than carbonates [30]. The preferential formation of bicarbonates rather than carbonates in the presence of  $\text{H}_2\text{O}$  upon  $\text{CO}_2$  chemisorption gives rise to a different interaction with the catalyst, which improves its chemisorption capacity towards carbon based species. Thus, the m/z 18 peak in the  $300\text{--}375^\circ\text{C}$  range observed in the experiment with  $\text{H}_2\text{O}$  saturation, which is assigned to  $\text{H}_2\text{O}$  occluded inside the tunnels, is not visible upon  $\text{CO}_2 + \text{H}_2\text{O}$  co-chemisorption, suggesting

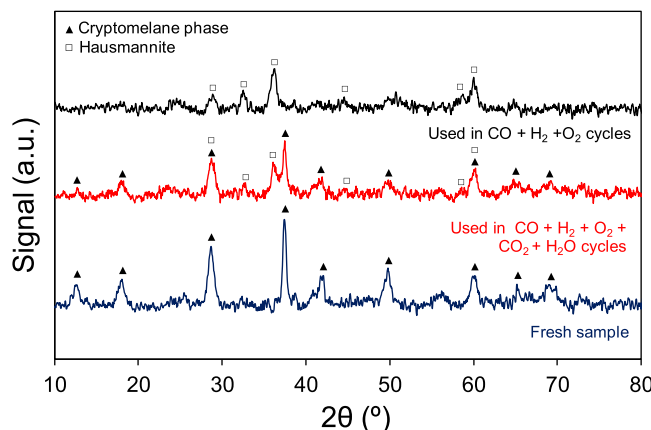


**Fig. 4.** XRD diffraction patterns for the CuO/Cryptomelane catalysts. Caption: (□) Cryptomelane: JCPDS card no. 29-1020; (▲)Hausmannite: JCPDS card no. 24-0734.

that  $\text{H}_2\text{O}$  is instead forming bicarbonate intermediates that cannot enter the narrow pores of the structure.

As a conclusion, TPD experiments have shown the synergistic effect between  $\text{CO}_2$  and  $\text{H}_2\text{O}$  towards the formation of chemisorbed species, which can be critical in the catalytic process. These TPD results (Fig. 3) are in agreement with the observed catalytic activities during the first cycle of CO-PROX experiments performed under different gas mixtures (Fig. 1), where  $\text{CO}_2$  has almost no influence,  $\text{H}_2\text{O}$  inhibits the activity by blocking active sites and/or decreasing oxygen vacancies and  $\text{CO}_2 + \text{H}_2\text{O}$  inhibit in higher extent by means of forming a larger amount of chemisorbed species with stronger interaction with cryptomelane. However, this negative effect of  $\text{CO}_2$  and  $\text{H}_2\text{O}$  co-chemisorption during the first cycle of catalytic tests (see Fig. 2) becomes positive effect in further cycles, and the reasons are discussed in the coming section.

### 3.3. Characterisation of fresh and used catalysts

Fig. 4 shows X-Ray diffraction patterns for the fresh CuO/Cryptomelane catalyst and once used in four consecutive reactions with  $\text{CO} + \text{H}_2 + \text{O}_2 + \text{CO}_2 + \text{H}_2\text{O}$  and with  $\text{CO} + \text{H}_2 + \text{O}_2$ . In all cases, the CuO tenorite diffraction peaks are not distinguished, but important changes in the diffraction pattern of the cryptomelane support are observed in the fresh and used samples. The X-Ray diffraction patterns shown in Fig. 4 prove that the deactivation of the CuO/Cryptomelane catalyst depends on the reaction gas mixture composition. Thus, once the catalyst was used in CO-PROX cycles in absence of  $\text{CO}_2$  and  $\text{H}_2\text{O}$ , the main crystallite phase is not cryptomelane, but hausmannite ( $\text{Mn}_3\text{O}_4$ ). This indicates that the strongly reductive environment of the CO-PROX reaction at the maximum temperature is able to reduce the manganese in the cryptomelane ( $\text{K}_x\text{Mn}_8\text{O}_{16-x}$ ) structure up to some extent. In our previous work [24], we discussed the deactivation process and the strategies of regeneration of the CuO/Cryptomelane catalyst in CO-PROX reaction. This study concluded that the catalytic activity of CuO/Cryptomelane was partially recovered by reoxidation between CO-PROX cycles at  $400^\circ\text{C}$  in  $\text{O}_2$  atmosphere. In addition, the presence of CuO nanoparticles on the surface was critical for the catalyst performance, which improved its catalytic activity when comparing to raw cryptomelane, but the stability was dramatically affected during the reactions. This work determined that with CuO, the reducibility of the catalyst was enhanced, and thus, its catalytic activity, but also the susceptibility to deactivation by reduction under CO-PROX conditions. However, despite the reoxidation treatments between cycles, it was not possible to restore completely the original catalytic activity, as a consequence of the partial collapse of cryptomelane structure by means of K segregation and sintering

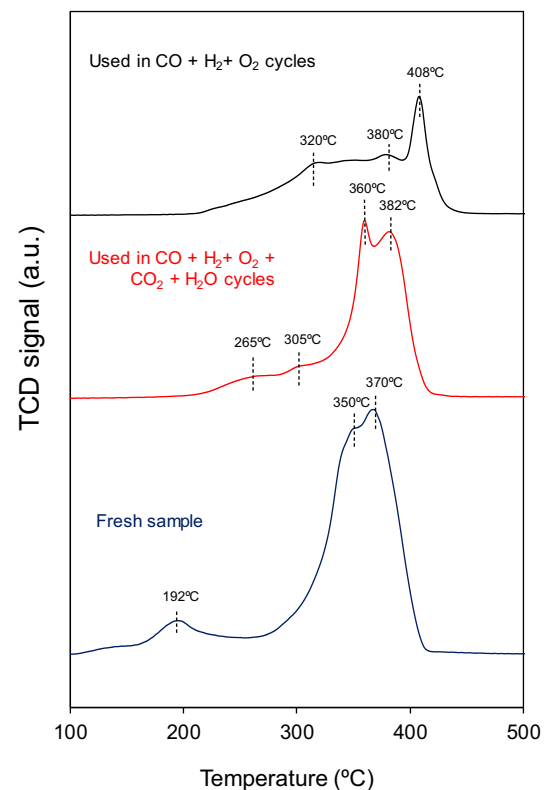


**Fig. 5.**  $\text{H}_2$ -TPR results for the CuO/Cryptomelane samples. 40 mg of catalyst, 40 ml/min 5%  $\text{H}_2$ /Ar,  $10^\circ\text{C}/\text{min}$ .

of CuO nanoparticles by means of the high temperature reached during such regeneration procedures.

In the present work, the regeneration issues are not taken into account, and the catalyst was tested during four reaction cycles without pretreatment between them in all the series conducted. According to Fig. 4, CuO/Cryptomelane catalyst is less damaged after used in reaction when  $\text{CO}_2$  and  $\text{H}_2\text{O}$  are present in the gas mixture, as cryptomelane peaks are still observed in the diffractogram. Then, the better performance after several uses in these conditions is necessarily associated to the catalyst stability and, consequently, reutilisation, aspects that have been studied for the first time in Cryptomelane-based catalysts under real CO-PROX reaction.

The  $\text{H}_2$ -TPR characterisation of the CuO/Cryptomelane catalyst, both fresh and used, evidence as well a higher stability during CO-PROX experiments performed with  $\text{CO}_2 + \text{H}_2\text{O}$  in the feed (results shown in Fig. 5), which is in agreement with the XRD characterisation.

It is well known that cryptomelane presents a  $\text{H}_2$  reduction profile which is based on multiple reduction steps until the final state of 2+ for manganese [19]. The presence of copper oxide modifies the reduction profile observable by the shift towards lower temperatures, produced by means of a synergistic effect between Cu and Mn. As well, the CuO present is also more easily reduced when it is finely dispersed onto cryptomelane support, when comparing to CuO bulk [24]. Hence, in fresh CuO/Cryptomelane can be distinguished a reduction peak with maxima at  $192^\circ\text{C}$ , which corresponds to the anticipated reduction of the CuO dispersed phase. This reduction peak is characteristic from the initial dispersion of CuO present in the catalyst at the beginning of the reaction. This CuO reduction peak is not discernible in the profiles for the used samples, which is shifted towards higher temperatures and overlapped under the reduction of bulk manganese, giving rise to the mixed reduction peaks centred between  $265^\circ\text{C}$  and  $320^\circ\text{C}$  in the used samples. This suggests that, under CO-PROX reaction con-

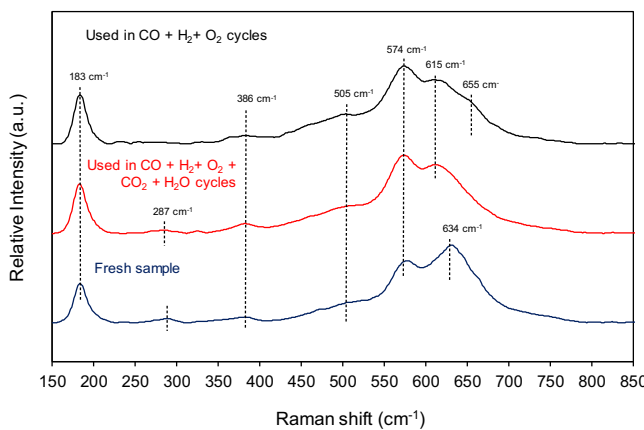


**Fig. 6.** Raman spectra of the fresh and used samples for CuO/Cryptomelane catalyst.

ditions, the CuO phase is partially sintered, lowering the Cu-Mn interaction [33], or reduced to a degree.

Nevertheless, the most explicit differences between the reduction profiles are relative to the reduction process for manganese in cryptomelane. The H<sub>2</sub> reduction profile of the catalysts used in CO-PROX experiments performed with CO<sub>2</sub> and H<sub>2</sub>O in the feed is qualitatively similar to the one for the fresh sample, but with lower area. The two main peaks observed in these profiles are assigned to the reduction of cryptomelane in two steps: (i) to Mn<sub>2</sub>O<sub>3</sub>/Mn<sub>3</sub>O<sub>4</sub>; (ii) to MnO. On the contrary, the H<sub>2</sub> reduction profile of the sample tested in CO-PROX experiments in absence of CO<sub>2</sub> and H<sub>2</sub>O presents totally different shape. The sharp peak centred at 408 °C is an evidence of the loss of Cu-Mn interaction and of the formation of Mn<sub>3</sub>O<sub>4</sub>, which is reduced in one step to MnO.

As a conclusion, H<sub>2</sub>-TPR characterisation confirms the greater stability of CuO/Cryptomelane during CO-PROX reactions performed with CO<sub>2</sub>+H<sub>2</sub>O in the feed, which presents partial degradation but keeps cryptomelane integrity up to an extent, which is not shown by the sample tested in CO-PROX experiments under the CO<sub>2</sub>- and H<sub>2</sub>O-free stream.

Raman spectra compiled on Fig. 6 are consistent with these conclusions, and also support the higher stability of the CuO/Cryptomelane catalyst during the CO-PROX experiments performed with CO<sub>2</sub> and H<sub>2</sub>O in the feed. The interpretation of the entire Raman spectra for cryptomelane-based crystalline structure is not trivial, as well as for the wide range of existing manganese oxides [34,35]. Cryptomelane is based on a body-centred tetragonal structure with space group I4/m [36] and its Raman spectrum features four main contributions at 183, 386, 574 and 634 cm<sup>-1</sup>, regarding the Mn-O vibrations within the MnO<sub>6</sub> octahedral double chains, along with some weak bands recorded at 287 and 505 cm<sup>-1</sup> [37]. Particularly, the low frequency Raman band at 183 cm<sup>-1</sup> has been assigned to an external vibration derived from the translational motion of the MnO<sub>6</sub> octahedra and the Raman band at 386 cm<sup>-1</sup> has been attributed to the Mn-O bending vibrations. On the other hand, the bands at 574 and 634 cm<sup>-1</sup> are due to symmetrical Mn-O vibrations, being assigned to vibrations in the along direction of the MnO<sub>6</sub> octahedral double chains, and in the perpendicular direction, respectively. Thus, the broadening, relative intensity and definition of the latter can be an indicative of the degree of development of the (2 × 2) tunnelled structure.

In the case of fresh CuO/Cryptomelane, the bands at 574 and 634 cm<sup>-1</sup> are not well defined, evidencing a poor crystallinity, as well as the relative intensities show a short length of nanofibers but a good definition of 2 × 2 channel size [35]. Attending to the used samples, the Raman spectra presents some differences between these bands in terms of Raman shift and relative intensities, which

is consistent with changes in the crystalline periodicity of cryptomelane phase, and the connection between the MnO<sub>6</sub> octahedra. In both cases, the band located at the 634 cm<sup>-1</sup> is shifted towards lower wavenumber, up to 615 cm<sup>-1</sup>, which can be associated to a higher Mn<sup>3+</sup>/Mn<sup>4+</sup> ratio in the network formed by MnO<sub>6</sub> octahedra [38,39]. Additionally, there can be discerned a shoulder at 655 cm<sup>-1</sup> in the CuO/Cryptomelane sample used in CO-PROX cycles in absence of CO<sub>2</sub>+H<sub>2</sub>O, that can be ascribed as the band characteristic for the symmetric stretching of Mn-O lattice for Mn<sub>3</sub>O<sub>4</sub> [40].

Thus, Raman characterisation suggests that used samples are based on a distorted cryptomelane structure formed by MnO<sub>6</sub> octahedra whose manganese has in average a more reduced oxidation state compared to the fresh sample. The reduction of manganese in the cryptomelane structure is possible by means of the formation of O<sup>2-</sup> vacancies and/or by the insertion of a greater proportion of K species in the intratunnel space. However, such reduction cannot overcome certain boundaries due to the electrostatic repulsion of the hosted K species, which may provoke a segregation into Mn<sub>3</sub>O<sub>4</sub> and a K-enriched cryptomelane phases [31]. Comparing both used samples, Raman characterisation evidences a higher development of Mn<sub>3</sub>O<sub>4</sub> phase in the sample used in absence of CO<sub>2</sub> and H<sub>2</sub>O in the catalytic tests.

In conclusion, the better performance of CuO/Cryptomelane catalyst after several CO-PROX experiments performed in the presence of CO<sub>2</sub> and H<sub>2</sub>O is related to its enhanced stability. In absence of CO<sub>2</sub> and H<sub>2</sub>O in the CO-PROX reaction feed, the catalyst is reduced leading to the formation of the phase Mn<sub>3</sub>O<sub>4</sub>, which decreases the catalytic activity up to a steady level. On the contrary, when CO<sub>2</sub> and H<sub>2</sub>O are present in the CO-PROX feed, their chemisorption maintains the tunnelled structure of cryptomelane.

#### 4. Conclusions

The catalytic activity of CuO/Cryptomelane for the preferential oxidation of CO in H<sub>2</sub>-rich streams has been studied in the absence and presence of H<sub>2</sub>O and CO<sub>2</sub>, and the following conclusions can be summarised:

For fresh CuO/cryptomelane catalyst, the presence of CO<sub>2</sub> and/or H<sub>2</sub>O in the CO-PROX feed partially inhibits CO oxidation due to chemisorption of H<sub>2</sub>O and CO<sub>2</sub> on the catalyst. H<sub>2</sub>O chemisorption on CuO/Cryptomelane is stronger than CO<sub>2</sub> chemisorption and simultaneous CO<sub>2</sub> and H<sub>2</sub>O feed has a synergistic effect that enhances co-adsorption.

On the contrary, the presence of CO<sub>2</sub>+H<sub>2</sub>O in the CO-PROX reaction mixture has a positive effect in the CuO/Cryptomelane stability upon several consecutive reaction cycles in the 25–200 °C range.

XRD showed that CO<sub>2</sub>+H<sub>2</sub>O co-chemisorption partially prevents catalyst deactivation due to cryptomelane reduction to hausmannite (Mn<sub>3</sub>O<sub>4</sub>) under the strongly reductive environment of the CO-PROX reaction. Additionally, H<sub>2</sub>-TPR and Raman spectroscopy characterisation support that the cryptomelane structure is less damaged under CO-PROX conditions in the presence of CO<sub>2</sub> and H<sub>2</sub>O than in the absence of these species.

Therefore, this greater stability of CuO/Cryptomelane in realistic conditions (CO<sub>2</sub> and H<sub>2</sub>O presence) is eventually minimising the catalyst deactivation in CO-PROX reaction cycles, and leads to the best catalytic performance after 4 cycles of reaction, which is a very interesting peculiarity of this material for the studied application.

#### Acknowledgements

Authors thank the financial support from Generalitat Valenciana (Project PROMETEOII/2014/010), Spanish Ministry of Economy and Competitiveness (Projects MAT2014-61992-EXP and CTQ2015-

67597-C2-2-R), Spanish Ministry of Education, Culture and Sports (grant FPU14/01178) and UE (FEDER funding).

## References

- [1] T. Choudhary, *Catal. Today* 77 (2002) 65–78.
- [2] A.F. Ghenciu, *Curr. Opin. Solid State Mater. Sci.* 6 (2002) 389–399.
- [3] E.D. Park, D. Lee, H.C. Lee, *Catal. Today* 139 (2009) 280–290.
- [4] B.C. McLellan, G.D. Corder, A. Golev, S.H. Ali, *Procedia Environ. Sci.* 20 (2014) 280–287.
- [5] K. Ramesh, L. Chen, F. Chen, Y. Liu, Z. Wang, Y.F. Han, *Catal. Today* 131 (2008) 477–482.
- [6] S. Veprek, *J. Catal.* 100 (1986) 250–263.
- [7] A. Marinou, M. Raceanu, C. Cobzaru, C. Teodorescu, D. Marinescu, A. Soare, M. Varlam, *React. Kinet. Mech. Catal.* 112 (2014) 37–50.
- [8] C.-H. Chen, S.L. Suib, *J. Chin. Chem. Soc.* 59 (2012) 465–472.
- [9] R.N. DeGuzman, Y.F. Shen, E.J. Neth, S.L. Suib, C.L. O'Young, S. Levine, J.M. Newsam, *Chem. Mater.* 6 (1994) 815–821.
- [10] S.L. Suib, *J. Mater. Chem.* 18 (14) (2008) 1623–1631.
- [11] G.G. Xia, Y.G. Yin, W.S. Willis, J.Y. Wang, S.L. Suib, *J. Catal.* 185 (1999) 91–105.
- [12] W.Y. Hernández, M.a. Centeno, F. Romero-Sarria, S. Ivanova, M. Montes, J.a. Odriozola, *Catal. Today* 157 (2010) 160–165.
- [13] X. Chen, Y.-F. Shen, S.L. Suib, C.L. O'Young, *Chem. Mater.* 14 (2) (2002) 940–948.
- [14] V.P. Santos, S.a C. Carabineiro, J.J.W. Bakker, O.S.G.P. Soares, X. Chen, M.F.R. Pereira, J.J.M. Órfão, J.L. Figueiredo, J. Gascon, F. Kapteijn, *J. Catal.* 309 (2014) 58–65.
- [15] R. Jothiramalingam, B. Viswanathan, T.K. Varadarajan, *Mater. Chem. Phys.* 100 (2006) 257–261.
- [16] W.Y. Hernández, M.a. Centeno, S. Ivanova, P. Eloy, E.M. Gaigneaux, J.a. Odriozola, *Appl. Catal. B Environ.* 123–124 (2012) 27–35.
- [17] Y. Shen, S.L. Suib, C.L. O'Young, *J. Catal.* 161 (1996) 115–122.
- [18] E.C. Njagi, H.C. Genuino, C.K. King'Ondu, C.H. Chen, D. Horvath, S.L. Suib, *Int. J. Hydrogen Energy* 36 (2011) 6768–6779.
- [19] W. Gac, *Appl. Catal. B Environ.* 75 (1-2) (2007) 107–117.
- [20] M. Özacar, A.S. Poyraz, H.C. Genuino, C.-H. Kuo, Y. Meng, S.L. Suib, *Appl. Catal. A Gen.* 462–463 (2013) 64–74.
- [21] J. Chen, J. Li, H. Li, X. Huang, W. Shen, *Microporous Mesoporous Mater.* 116 (2008) 586–592.
- [22] T.I.M. Martínez, F. Romero-Sarria, W.Y. Hernández, M.a. Centeno, J.a. Odriozola, *Appl. Catal. A Gen.* 423–424 (2012) 137–145.
- [23] X.-S. Liu, Z.-N. Jin, J.-Q. Lu, X.-X. Wang, M.-F. Luo, *Chem. Eng. J.* 162 (1) (2010) 151–157.
- [24] A. Davó-Quiñonero, M. Navlani-García, D. Lozano-Castelló, A. Bueno-López, *Catal. Sci. Technol.* 6 (14) (2016) 5684–5691.
- [25] D. Gamarra, A. Martínez-Arias, *J. Catal.* 263 (2009) 189–195.
- [26] G.K. Reddy, P.G. Smirniotis, *Water Gas Shift Reaction: Research Developments and Applications*, 2015.
- [27] Y.F. Shen, R.P. Zerger, R.N. DeGuzman, S.L. Suib, L. McCurdy, D.I. Potter, C.L. O'Young, *Science* 5107 (1993) 511–515.
- [28] A. Martínez-Arias, D. Gamarra, A. Hungría, M. Fernández-García, G. Munuera, A. Hornés, P. Bera, J. Conesa, A. Cámaras, *Catalysts* 3 (2013) 378–400.
- [29] F. Mariño, C. Descorme, D. Duprez, *Appl. Catal. B Environ.* 58 (2005) 175–183.
- [30] A. Davó-Quiñonero, M. Navlani-García, D. Lozano-Castelló, A. Bueno-López, J.A. Anderson, *ACS Catal.* 6 (3) (2016) 1723–1731.
- [31] T. Gao, P. Norby, *Eur. J. Inorg. Chem.* (28) (2013) 4948–4957.
- [32] N. Kijima, H. Yasuda, T. Sato, Y.J. Yoshimura, *Solid State Chem.* 159 (2001) 94–102.
- [33] K. Qian, Z. Qian, Q. Hua, Z. Jiang, W. Huang, *Appl. Surf. Sci.* 273 (2013) 357–363.
- [34] C. Julien, M. Massot, R. Baddour-Hadjean, S. Franger, S. Bach, J.P. Pereira-Ramos, *Solid State Ionics* 159 (2003) 345–356.
- [35] T. Gao, H. Fjellvåg, P. Norby, *Anal. Chim. Acta* 648 (2009) 235–239.
- [36] J. Vicat, E. Fanchon, P. Strobel, D. Tran Qui, *Acta Crys. Sect. B* 42 (1986) 162–167.
- [37] T. Gao, M. Glerup, F. Krumeich, R. Nesper, H. Fjellvåg, P.J. Norby, *Phys. Chem. C* 112 (34) (2008) 13134–13140.
- [38] M.-C. Bernard, A.H.-L. Goff, *J. Electrochem. Soc.* 140 (11) (1993) 3065–3070.
- [39] F. Buciuman, F. Patcas, R. Craciun, D.R.T. Zahn, *Phys. Chem. Chem. Phys.* 1 (1999) 563–569.
- [40] F. Kapteijn, L. Singoredjo, A. Andreini, J.A. Moulijn, *Appl. Catal. B Environ.* 3 (1994) 173–189.